01 Jan 1975

Double Reflection Dips from Grating Ruled Semiconductors

L. F. Teng

Ralph William Alexander
Missouri University of Science and Technology, ralexand@mst.edu

Robert John Bell
Missouri University of Science and Technology

B. Fischer

phys. stat. sol. (b) 68, 513 (1975)

Subject classification: 20.1; 6; 13.5.2; 22.2.1; 22.2.3

Materials Research Center and Physics Department, University of Missouri-Rolla, Rolla (a), and Max-Planck-Institut für Festkörperforschung, Stuttgart, and Thomas J. Watson Laboratories, International Business Machine Corporation, Yorktown Heights, New York (b)

Double Reflection Dips from Grating Ruled Semiconductors

By

L. F. Teng (a), R. W. Alexander, Jr. (a), R. J. Bell (a), and B. Fischer (b)

The double reflectivity dips, previously observed by Fischer et al. and Anderson et al., which appeared in the reflection spectra of grating surfaces on the Te-doped semiconductors GaAs and InSb around both the plasmon and phonon frequencies have been measured in more detail. In the plasmon region, several possible explanations of the phenomenon are discussed, but the favored explanation involves surface damage. A simple two-region reflectivity equation checked with a rigorous grating theory is proposed and is shown to fit the data well.

Die bereits von Fischer et al. und Anderson et al. beobachteten doppelten Minima in den Reflexionsspektren der Gitteroberflächen von mit Te dotiertem GaAs und InSb nahe den Plasmon- und Phononfrequenzen wurden ausführlich gemessen. Für den Plasmonbereich werden mehrere mögliche Erklärungen des Phänomens diskutiert, jedoch wird eine Erklärung, die mit Oberflächenschäden zusammenhängt, bevorzugt. Es wird eine einfache Gleichung für die Reflexion in zwei Bereichen vorgeschlagen, die mit einer strengen Theorie geprüft wird. Es wird Übereinstimmung mit den Meßdaten gefunden.

1. Introduction

Through the studies of surface plasmons on the Te-doped semiconductors GaAs and InSb with gratings ruled on the surfaces Marschall et al. [1] discovered a new phenomenon occurring in the reflection spectra. Near the plasmon and phonon frequencies they found double dips in the reflectance under specific conditions for some of their semiconductor samples [2]. In their experiments, the electric field $\boldsymbol{E}$ of the polarized light was always parallel to the incident plane. The double dips in the reflectance appeared for some samples in the plasmon region when the grating grooves were turned parallel to $\boldsymbol{E}$. While in the phonon region, the results were just the opposite; the double dip existed when the grating grooves and $\boldsymbol{E}$ were perpendicular but did not exist when they were parallel to each other. Tentative explanations were made in their report [2] to the effect that the plasmon double dips were due to a fraction of the bulk plasmon resonance adding to the "plasma edge" formed by individual electron oscillation and that the phonon double dip was a result of the coupled modes of surface-plasmons and bulk phonons. More evidence and discussion show that the bulk plasmon resonance assumption cannot explain the phenomenon for several reasons.

(i) The "plasma edge" of the individual electron oscillations is equal to the plasmon resonance frequency ω_p; so two separate minima should not appear near ω_p (see for example [3]).

(ii) As to be described in this paper, double dips also occur when $\boldsymbol{E}$ is perpendicular to the incident plane at almost normal incident angles. In this orientation, it is impossible to excite a bulk plasmon resonance [4].

(iii) Finally, the double dips do not occure for smooth surface samples, and there is no theory or reasonable assumption to show the necessity of a grating to excite the bulk plasmon resonance.

In this paper, we will report new experiments and will briefly discuss some other possible explanations to the problem. Finally to fit the data, we will present a very simple reflectance equation which is supported with a more rigorous theory. A brief discussion and identification for the extra dip in the phonon region will also be made.

2. Experiment and Discussion in the Plasmon Regions

The grating Te-doped semiconductor samples GaAs and InSb have been described by Fischer et al. previously [1, 2]. Sample group A was GaAs, with doped electron concentration $n = 4.2 \times 10^{18}$ electrons/cm^3; group B was InSb, $n = 1.1 \times 10^{18}$ electrons/cm^3; group C was InSb, $n = 4.7 \times 10^{17}$ electrons/cm^3. A10, A20, A30, A40 denote sample group A with grating constants $d = 10$, 20, 30, and 40 μm, respectively. The same notation expressing the samples of different grating constants was also used for groups B and C. The incidence radiation was almost normal to the sample (incident angle $< 10°$). Double beam spectra were taken and the reflectivity shown in the spectra is of an arbitrary scale. A summary of the data obtained is listed as Table 1.

Table 1

Observed reflectivity minima near the plasma frequencies. The frequency of the maximum between the minima is also listed

sample	double dips ?	E_{pp}*) or E_{sp}**) max. and min. frequency (cm^{-1})			E_{ps} min. frequency (cm^{-1})
		1st min.	max	2nd min.	
A10	S*) **)	560*) **)	672	740	680*) **)
A20	W*)	640*)	672	725	—
A30	N*) **)	720*) **)			720*) **)
A40	N**)	720**)			720**)
B10	S*), Y**)	620*) **)	670	770	740**)
B20	N**)	770**)			750**)
B30	N**)	760**)			760**)
C10	W**)	420**)	480	540	450**)
C20	N**)	450**)			450**)
C30	N**)	450**)			450**)

*) Fischer's data; **) current data.
S: yes, strong; W: yes, very weak; Y: yes, not strong; N: no.
E_{ps}: $\boldsymbol{E}$ parallel to incident plane and $\boldsymbol{E}$ perpendicular to grating grooves. The bulk plasmon frequency is approximately equal to the minimum frequency of E_{ps}.
E_{pp}*): $\boldsymbol{E}$ parallel to incident plane and $\boldsymbol{E}$ parallel to grating grooves. (By Fischer)
E_{sp}**): $\boldsymbol{E}$ perpendicular to incident plane and $\boldsymbol{E}$ parallel to grating grooves. (By the present authors)

Sample A10 shows the double dip effect most strongly. Fig. 1 is a comparison of the reflectances for the electric field, $\boldsymbol{E}$, perpendicular (curve a) and parallel (curve b) to the incident plane for this sample. Also shown in the figure is the reflectance from the smooth surface (curve c) which resembles the $\boldsymbol{E}$ parallel case of curve b. Fig. 2 makes the same comparisons for samples B10 and C10. Both samples are sensitive to the polarization of the incident field. The higher reflectivity for the $\boldsymbol{E}$ parallel field is partly due to instrumental effects. Fig. 3 shows the behavior with different grating constants ($d = 10$, 20, and 30 μm) for the samples A10, A20, and A30. Fig. 4 shows the double dips of what we will call the standard reference case (curve a, same curve from Fig. 1, curve a), compared to the cases of larger incident angle (curve b), different grating groove orientation (curve c), and a narrower band of incident wavelengths (curve d) obtained by using a band pass filter cutting out the frequency beyound 1000 cm^{-1} (curve d). For all these spectra, the essential features remain the same except the depth of the two dips differ slightly. An attempt was made to get the higher order diffraction spectra for $d = 20$, 30, and 40 μm, but not enough signal was detected. For $d = 10$ μm, the grating constant is smaller than the wavelength in the double dip region, so no diffracted order exists.

A summary of the experimental results for the double dips near the plasma frequency is as follows:

1. A double dip occurs in some Te-doped semiconductors on both sides of the plasmon frequency ω_p. The frequency of the maximum is located around the

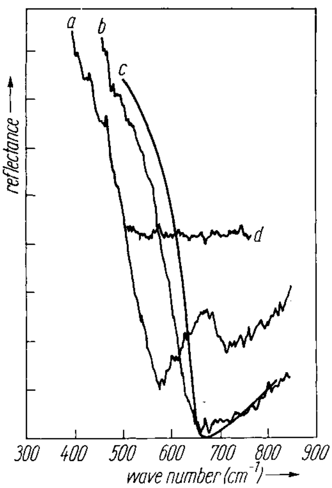

Fig. 1

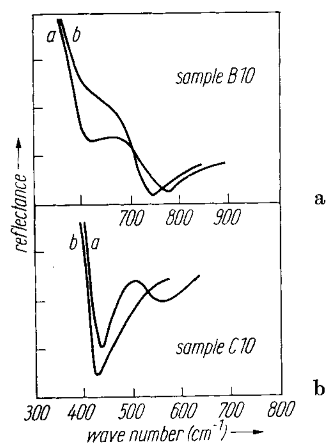

Fig. 2

Fig. 1. Reflection spectra of sample A10 (GaAs, $n = 4.2 \times 10^{18}$ electrons/cm^3, $d = 10$ μm). Incident angle $\approx 6°$. (a) $\boldsymbol{E}$ perpendicular to the incident plane and parallel to the grating grooves; (b) $\boldsymbol{E}$ parallel to the incident plane and perpendicular to the grating grooves; (c) spectrum of the sample with smooth surface ($\boldsymbol{E}$ perpendicular to the incident plane); (d) spectrum of a mirror background ($\boldsymbol{E}$ perpendicular to the incident plane)

Fig. 2. Reflection spectra of samples, incident angle $\approx 6°$; a) sample B10 (InSb, $n = 1.1 \times 10^{18}$ electrons/cm^3, $d = 10$ μm), orientation same as Fig. 1 for curve a and b; b) sample C10 (InSb, $n = 4.7 \times 10^{17}$ electrons/cm^3, $d = 10$ μm), orientation as in Fig. 1 for curves a and b

middle point between these two dips, and may be larger or smaller than ω_p (Fig. 1 and 2).

2. For an appropriate sample with a large enough groove width to grating constant ratio, a double dip occurs at all except one of the possible combinations of the orientations of the electric field $\boldsymbol{E}$, the incident plane, and the grating grooves. The exception for which a double dip does not appear is with $\boldsymbol{E}$ parallel to the incident plane and perpendicular to the grating grooves, which is the case for which a surface wave may be excited. This suggests that a surface wave may have the effect of eliminating the double dips (Fig. 1, 2, and 4).

3. As a special case of point 2 above, the double dip occurs almost independent of the orientation of the grating grooves if the electric field $\boldsymbol{E}$ is perpendicular to the incident plane. Except for some change of the shape and the relative depth of the two dips, the positions of the two dips and the maximum remain essentially the same (Fig. 4, curve c).

4. The double dip occurs only for samples with relatively small grating constants. Except for one sample with $d = 20\ \mu m$ (which shows a much smaller effect) all samples with $d > 10\ \mu m$ show no double dips. This suggests that the effect is dependent on the grating constants (Fig. 3).

5. The double dip occurs only for samples having a grating on the surface. It does not appear on a smooth or an irregularly rough surface.

6. The double dips do not depend on the incident angle of the light (Fig. 4, curve b).

7. No systematic effects were found from the spectra for various kinds of doped semiconductors or different carrier concentrations.

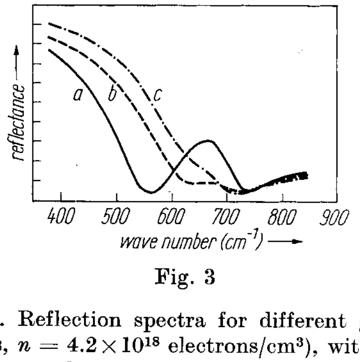

Fig. 3

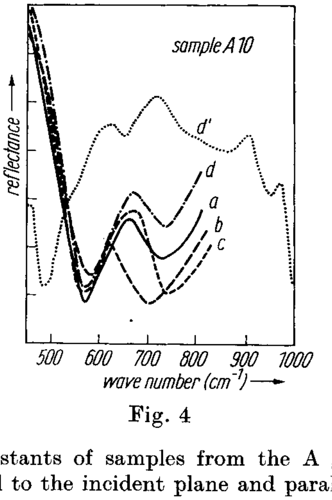

Fig. 4

Fig. 3. Reflection spectra for different grating constants of samples from the A group (GaAs, $n = 4.2 \times 10^{18}$ electrons/cm^3), with $\boldsymbol{E}$ parallel to the incident plane and parallel to the grating grooves: (a) $d = 10\ \mu m$; (b) $d = 20\ \mu m$; (c) $d = 30\ \mu m$

Fig. 4. Reflection spectra for different optical conditions A10 (GaAs, $n = 4.2 \times 10^{18}$ electrons/cm^3, $d = 10\ \mu m$) but in every case with $\boldsymbol{E}$ perpendicular to the incident plane and parallel to the grating grooves except as noted. (a) same curve as Fig. 1, curve a; (b) incident angle $\approx 45°$; (c) grating grooves rotated an angle $\approx 60°$ with respect to (a); (d) a band pass filter placed in front of the sample; (d′) spectrum of the filter used for (d) only. (Note the cut-off of the intensity beyond 1000 cm^{-1})

Several possibilities were tried to explain this double dip phenomenon. Among those were an emission effect around the plasmon frequency producing a peak in reflectivity where a minimum was expected otherwise. This concept included the excitation and subsequent emission of the radiative and nonradiative surface plasmon modes. The non-radiative surface modes cannot couple with photons directly. With the help of the grating on the sample surface, however, these modes can emit light as well as be excited by it. Both radiative and non-radiative modes can radiate light at the frequencies consistent with our data but failed in other important conditions: (i) the surface plasmon can only couple with light polarized parallel to the incident plane; (ii) the peak position depends on the incident angle of light; (iii) according to Ferrell [6], the photon intensity and the line breadth of the emitted light from a radiative plasmon should have a characteristic angular dependence, $I(\theta) \sim \cos\theta/[1 + (\theta_0/\theta)^2]$ where θ_0 is a constant and θ is the angle of emission measured from the surface normal; (iv) in the non-radiative case, it should depend on the orientation of the grating grooves [7]; and (v) the shape of peaks appearing in all experiments performed by Ritchie et al. [8, 9] are high and sharp. All of the above features [(i) to (v)] have not appeared in our double dip spectra, and therefore surface plasmon radiation must be ruled out as explaining the effects.

Other possibilities such as wave transformation processes [10] band effects [8, 9, 11] and "*P*-anomalies" [12] were also considered and eliminated. An experiment was performed to test the nonlinear transformation process in which absorption of light at frequency $2\omega_p$ would produce emission at ω_p. A silicon filter was used to cut-off sharply the incident light beyond 1000 cm^{-1}. With the filter there was no light at $2\omega_p$ ($\omega_p = 680$ cm^{-1} for sample A, see Fig. 4, curve d and d′) shining on the sample. Nothing other than the overall intensity changed in this experiment, so that such a transformation process cannot be responsible for the effect. The band effect was also ruled out although for sample A10, the data coincidently fitted to the band gap. Because no surface waves were excited in the double dip orientations, no band gap (which could be produced from the periodicity introduced with the grating) arose. To have "*P*-anomalies", the depth of the grating grooves should be at least larger than 3 μm according to Hessel and Oliner's [13] theory, which is not the case. The groove depth is about 1 μm as estimated from photomicrographs.

3. Rigorous Grating Theory and a Simple Reflectance Equation

3.1 Rigorous grating theory

We have derived a rigourous grating theory mainly following Neviere et al. [14]. For polarized light with wave vector $\boldsymbol{k}_0$, electric field $\boldsymbol{E}$ perpendicular to the incident plane and parallel to the grating grooves, and incident angle θ, the zeroth order reflectance can be shown to be [14]

$$R = |2ik_0T_{00}\cos\theta + 1|^2\,, \tag{1}$$

where T_{00} is the middle element on the diagonal of the infinite matrix

$$T = M_1M^{-1}\,. \tag{2}$$

M^{-1} is the inverse of the square matrix M which has been numerically shown not to be equal to zero within the region of interest. For rectangular gratings, M was defined in terms of the dielectric constants $\varepsilon(\omega)$, the grating constant d, the groove depth h, and k_0 with the aid of the following set of equations:

$$M \equiv M_2 + L_h M_1 \tag{3}$$

with

$$M_1 = M_{11} - M_{12} L_0$$

and

$$M_2 = M_{21} - M_{22} L_0 \,,$$

where

$$\begin{pmatrix} M_{11} & M_{12} \\ M_{21} & M_{22} \end{pmatrix} = \begin{pmatrix} I & I\Delta \\ A\Delta & I \end{pmatrix}^N . \tag{4}$$

I is the infinite unit matrix. A is a matrix with elements $a_{n,m} = -\alpha_{n-m} + \gamma_n^2 \delta_{n,m}$, where n and m are any integers from $-\infty$ to ∞; $\alpha_{n-m} = k_0^2 \varepsilon_{n-m}$, ε_{n-m} is the $(n-m)$-th Fourier component of the anticipated periodic dielectric function as one traverses horizontally from grating groove to grating groove; and γ_n is defined below. Vertically dividing the groove profile into N identical parts, one has each part of depth $\Delta = h/N$. For the numerical calculation $N = 4$ and 10 yielded about the same reflectances for $h = 1$ μm. L_0 and L_h are infinite diagonal matrices with $L_{0\,n,n} = i\beta_{k,3}$ and $L_{h\,k,k} = -i\beta_{k,1}$ with

$$\gamma_n = k_0 \sin\theta + nK, \quad K = \frac{2\pi}{d} \quad \text{and} \quad n = 0, \pm 1, \pm 2, \tag{5}$$

and

$$\beta_{n,1} = \sqrt{k_0^2 - \gamma_n^2} \quad \text{and} \quad \beta_{n,3} = \sqrt{\varepsilon k_0^2 - \gamma_n^2} . \tag{6}$$

$\varepsilon(\omega)$ is the bulk dielectric function of the material given by [15]

$$\varepsilon(\omega) = \varepsilon_\infty + \frac{\delta\varepsilon}{1 - \left(\dfrac{\omega}{\omega_0}\right)^2 - \dfrac{i\omega\Gamma}{\omega_0^2}} - \frac{\omega_p^2 \varepsilon_\infty}{\omega^2 + \dfrac{i\omega}{\tau}} , \tag{7}$$

where ε_∞ is the high frequency dielectric constant; ω_0 is considered to be the transverse optical mode frequency ω_{TO} when Γ, the damping parameter of the phonons is small; $\delta\varepsilon$ is the strength of the mode; $\omega_p^2 = 4\pi N e^2/(m^* \varepsilon_\infty)$ is the plasma frequency; N is the free carrier concentration with electron charge e and effective mass m^*; and τ is the collision time of the free carriers.

3.2 Computation from the rigorous theory

Using the equations from the rigorous grating theory presented in Section 3.1, the reflectance was calculated for the samples discussed previously. The parameters used are from Willardson and Beer's book [16], and McMahon's dissertation [17].

Only seven terms starting from the central $n = 0$, going to both positive and negative integers and terminating at $n = \pm 3$, were taken for the summations of the infinite series presented in Section 3.1. This series has been checked and found to converge rapidly for the grating constants used here. The N in (4) was taken to be 10, which is large enough for h to be in the range of micrometers.

The results of the calculation depend upon what is assumed for the dielectric functions. A rectangular grating is assumed in these calculations.

Case 1: Assume the dielectric function inside the lanes (the region labeled g in the insert figure of Fig. 5) of the grating region is the same as the bulk value

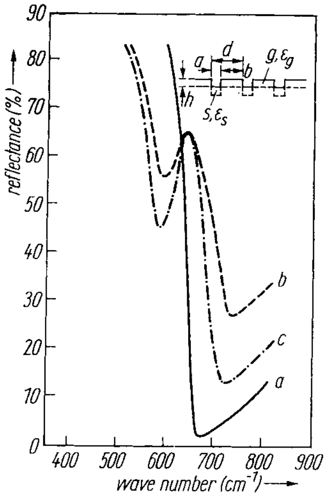

Fig. 5. Calculated reflection spectra for sample A10 from the rigorous grating theory. (a) $\varepsilon_g = \varepsilon_s = \varepsilon$, case 1; (b) $\varepsilon_g > \varepsilon$, $\varepsilon_s = \varepsilon$, case 2; (c) $\varepsilon_g > \varepsilon$, $\varepsilon_s < \varepsilon$, case 3.

of the material, i.e. $\varepsilon_g = \varepsilon$. No double dips appear in the reflectivity as shown in Fig. 5, curve a. Here the wavelength is larger than the grating constant, and no diffraction effects appear. The reflection in this case is almost the same as from a smooth surface.

Case 2: Assume $\varepsilon_g > \varepsilon$. This difference in the dielectric constant is due to the distortion of the electron density inside the grating region; so, the concentration of electrons as well as the damping inside this region is not the same as in the bulk. In this case, the double dip appears. By choosing suitable ω_{pg} (the plasma frequency in region g) for ε_g, the dip positions can be fitted. In Fig. 5, curve b, $\omega_{pg} = 520\ cm^{-1}$ is used for sample A10. The first and the second dips are at 590 and 735 cm^{-1}, respectively. Compared to the experimental values of 570 and 740 cm^{-1}, the discrepancies are less than 5%. Nevertheless, the calculated reflectivity, especially around the first dip position, is much higher than the experimental value.

Case 3: Gamon and Palik [18] in their recent paper pointed out that the carrier density, and hence the plasma frequency, near the surface is not the same as the bulk value for doped semiconductors InSb and GaAs. The variation is about ±7%. They did not mention the depth below the surface to which this variation extends: it might be only in the order of angströms. However, because of the damage inside the groove region, and also because of the distortion of electron density from the neighboring lanes, it is reasonable to make a further assumption that the dielectric function in the region s of the insert figure of Fig. 5 is not ε but $\varepsilon_s < \varepsilon$. Fig. 5, curve c is a plot for sample A10 based on this assumption by taking $\omega_{pg} = 520\ cm^{-1}$ for ε_g and $\omega_{ps} = 720\ cm^{-1}$ for ε_s, assuming a layer thickness of 1 μm on the groove surface. The positions of the dips fit the experimental data. The reflectivity is still too high, although better than the previous case.

The calculated results of samples B10 and C10 are similar to that of A10 described above. Just by choosing suitable values of ω_{pg} and ω_{ps}, the double dip positions can always be fitted within an accuracy of 5%. The reflectivities are higher than the experimental values. For large grating constants, the dielectric function ε_g inside the lane region approaches the bulk value ε because of less distortion of the electron densities, so the double dips will disappear and will reduce to a usual plasma dip.

These calculations were only for the special case in which grating grooves are parallel to the electric field $\boldsymbol{E}$ and perpendicular to the incident plane. For $\boldsymbol{E}$ parallel to the incident plane, or other orientations of the grating grooves, the situation will be much more complicated. The model described in the next section will cover these cases with a very simple argument.

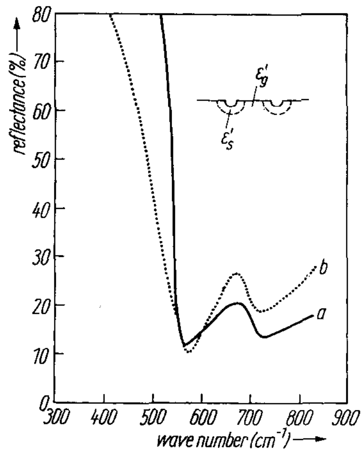

Fig. 6. (a) reflection spectrum calculated from the simple equation. (9) compared with (b) the experimental reflectivity of sample A10 for the E_{sp}**) case of Table 1

3.3 A simple reflectivity equation

The double dips, if they are due to the distortion of electron densities near the grating surface, can be always imagined as arising from the combination without interference of two reflectances. One reflectance has a dip at a higher, and the other has a dip at a lower frequency than the bulk plasma frequency. Looking at the insert of Fig. 6, the separate reflectances for the ε_s' and ε_g' regions can be calculated since the ionic part of the dielectric functions are the same and only the plasma frequencies and free carrier collision parameters differ in the two regions. The reflectance R_1 from the regions g can be calculated from [15]

$$R_1 = \frac{(\cos\theta - a)^2 + b^2}{(\cos\theta + a)^2 + b^2}, \tag{8}$$

where

$$\left.\begin{matrix} 2a^2 \\ 2b^2 \end{matrix}\right\} = [(\varepsilon_{g1}' - \sin^2\theta)^2 + \varepsilon_{g2}']^{1/2} \pm (\varepsilon_{g1} - \sin^2\theta)$$

with

$$\varepsilon_{g1}' = \operatorname{Re}[\varepsilon_g'(\omega)]\,,$$
$$\varepsilon_{g2}' = \operatorname{Im}[\varepsilon_g'(\omega)]\,.$$

R_2 from the region s can be similarly calculated. If interference is neglected because of the small grating constants compared to the wavelength, the total reflectance appearing in the spectrum can be written as

$$R = \frac{R_1A_1 + R_2A_2}{A_1 + A_2}, \tag{9}$$

where A_1 is the surface area of the lane portion and A_2 that of the groove portion. Fig. 6, curve a is a plot of R for $A_1:A_2 = 7:1$, $\omega_{pg}' = 525\ \text{cm}^{-1}$, $\omega_{ps}' = 710\ \text{cm}^{-1}$, and $1/\tau_g = 1/\tau_s = 1/\tau = 15\ \text{cm}^{-1}$ for sample A10. The τ's do not affect the dips much, and they were all taken to be equal for the sake of simplicity. Fig. 6, curve b is the experimental data. The dips and the maximum between them are almost coincident with the calculated values. The reflectivity magnitudes are more consistent too. Again, for samples B10 and C10, the fit can also be obtained just by choosing suitable values of ω'_{pg} and ω'_{ps}.

Not only the position and intensity of maximum and dips can be fitted well by this simple equation, but also all properties as summarized in the experimental results can be easily explained with a little argument.

The only orientation that does not show double dips is for $\boldsymbol{E}$ parallel to the incident plane and perpendicular to the grating grooves, which is the case that is supposed to have a surface wave excited by the grating. The absence of the double dips may be because any surface wave excitation causing a third dip lying between the double dips washes out the maximum between, or the absence might be because of the following reason. Referring to the insert figure of Fig. 5 in a bulk wave case, the oscillation of electrons at g is only a response to the light shining on g, and that at s is only a response of light shining on s. If the dielectric functions are different between regions g and s, and if interference effects can be ignored, the combination of the reflectance from these two points will appear as two dips. In case a surface wave is excited the oscillation of electrons in region g is not only the response of the light shining on g, but is also a response of the surface wave coming from regions s. Therefore, the difference of the dielectric function between those points will be averaged out.

3.4 Comparison of the simple reflectivity equation and the rigorous grating theory

Equation (9) of the last section agrees with the experiments and results from a very simple model. It is worthwhile to make the connection between the simple equation (9) and the rigorous grating theory results of equation (1) given in Section 3.1. Case 3 in Section 3.2 gave results very similar to the simple equation in Section 3.3. Both showed the double dips in the correct positions with almost the same value of parameters. The principal difference in the results of the two models is that the simple model can fit both the relative intensities of the double dips and the frequency of the maximum, while the rigorous grating theory only yielded the frequencies accurately. This may mean that the grating theory assumptions are not completely accurate because the factors affecting them are so complicated.

4. Double Dips around the Optical Phonon Frequency Region

Marschall et al. [2], besides the phonon–plasmon coupling minimum at $265\ \text{cm}^{-1}$, found around the optical phonon frequency region another dip at the frequency $\omega = 305\ \text{cm}^{-1}$ for the sample A10 (GaAs, $n = 4.2 \times 10^{18}$ electrons/cm^3 and $d = 10\ \mu\text{m}$). The depth of these two phonon region reflectivity dips is approximately the same, but the extra dip occurs only when $\boldsymbol{E}$ is parallel to the incident plane and perpendicular to the grating grooves, which is the case for which it is possible to excite a surface wave on the material. This phenomenon is absent in the other orientations in which only the bulk plasmon–bulk phonon coupled low frequency mode is observed. For the double dips, Fischer suggested an explanation that this is related to a coupled mode of surface plasmons and bulk phonons.

However, since the grating constant d equals $10\ \mu\text{m}$, the surface wave vector k from the relation $k = (\omega/c) \sin \theta + n 2\pi/d$ is always larger than $6280\ \text{cm}^{-1}$.

At this large k, no surface plasmon can be excited around the phonon region. So if this extra dip is a result of surface wave absorption, it can only be a surface phonon.

The longitudinal phonon frequency of GaAs [16] is $\omega_L = 297\ \text{cm}^{-1}$; then for large k, the surface phonon frequency is $\omega_{sL} \approx (1 + 1/\varepsilon_\infty)^{-1/2}\, \omega_L$, so that $\omega_{sL} = 284\ \text{cm}^{-1}$ for $\varepsilon_\infty = 10.9$. To find the reflection dip from this eigenfrequency, the exact approach involves grating theory. But instead, we will make estimations following Fischer's very simple method [1].

Cowan et al. [19] have shown that the excitation of a photon–surface plasmon–photon system is equivalent to a typical Lorentzian oscillator. Fischer assumed Lorentzian oscillators for his surface plasmons and got a fit to the reflectivity and dispersion curves. We used these Lorentzian oscillators contributing to the dielectric function $\varepsilon(\omega)$. For simplicity, we assumed that all parameters except the eigenfrequency are almost the same as the bulk values, and that nothing couples to this surface wave; then the reflection minimum will occur at the frequency ω_{dip}, such that $\text{Re}\,[\sqrt{\varepsilon(\omega_{\text{dip}})}] = 1$. By numerical methods, we find $\omega_{\text{dip}} = 307\ \text{cm}^{-1}$. This estimation fits the experimental value of $305\ \text{cm}^{-1}$.

5. Conclusions

Near the plasmon frequency, the best fit to the data is made by assuming, as shown in the insert figure of Fig. 5 or 7, that the dielectric function $\varepsilon_s (\varepsilon_s < \varepsilon)$ extends to a depth of a few micrometers and that there is no coupling to surface phonons. Since the character of a semiconductor usually changes dramatically with a few defects in the material, e.g. a huge change of conductivity with a small concentration of impurities, it is not unreasonable for the grating ruled in the surface to cause the results found in this study.

What was done in this work has been to make experimental measurements and to propose a simple model to explain almost all the experimental phenomena with an uncomplicated assumption.

Several points in this work should be emphasized:

(i) The reflectivities expected from two different bulk plasmons in the lane and the groove regions respectively were shown to appear as double dips only around the "plasma edge" region. In other frequency regions not near the "plasma edge" or the reststrahlen frequency, no difference appeared in the reflectivity between the smooth and the grating surfaces if no surface wave has been excited in those regions.

(ii) The double dip features were smeared out in the orientation for which surface plasmons can be excited as the surface waves cross the lane and groove strips with their different free carrier concentrations.

In the reststrahlen frequency region, the double dips are caused by 1. the low frequency bulk plasmon–bulk phonon coupled mode and 2. the surface phonons.

Acknowledgements

The work was partially supported by the NSF under contract number NSF GH 34551. One of us (R.W.A.) acknowledges a grant from the Research Corporation.

References

[1] N. Marschall, B. Fischer, and H. J. Queisser, Phys. Rev. Letters 27, 95 (1971).
[2] B. Fischer and N. Marschall, Proc. X. Internat. Conf. Phys. Semicond., Cambridge, Massachusetts 1970, Ed. S. P. Keller, J. C. Hensel, and F. Stern, U. S. AEC Division of Technical Information, Springfield, Va. 1970 (p. 845).
[3] C. Kittel, Introduction to Solid State Physics, 3rd ed., John Wiley & Sons, New York 1966 (p. 229).
[4] W. Steinmann, phys. stat. sol. **28**, 437 (1968).
[5] W. E. Anderson, R. W. Alexander, Jr., and R. J. Bell, Phys. Rev. Letters **27**, 1057 (1971).
[6] F. A. Ferrell, Phys. Rev. **111**, 1214 (1958).
[7] R. H. Y. Y. Teng and A. S. Karakashian, Phys. Rev. Letters **37A**, 27 (1971).
[8] J. J. Cowan, E. T. Arakawa, and R. H. Ritchie, The Surface Plasmon Resonance in Grating Diffraction, Oak Ridge National Laboratory Report, ORNL-TM-2615.
[9] R. H. Ritchie, E. T. Arakawa, J. J. Cowan, and R. N. Hamm, Phys. Rev. Letters **22**, 1530 (1968).
[10] A. Bianconi and M. Iannuzzi, Phys. Rev. Letters **27**, 932 (1971).
[11] J. J. Cowan and E. T. Arakawa, Z. Phys. **235**, 97 (1970).
[12] C. H. Palmer, J. Opt. Soc. Amer. **42**, 269 (1952).
[13] A. Hessel and A. A. Oliner, Appl. Optics **4**, 1275 (1965).
[14] M. Neviere, R. Petit, and M. Cadilhac, Opt. Commun. 8, 113 (1973).
L. F. Teng, Ph. D. Dissertation, University of Missouri-Rolla, 1974.
[15] R. J. Bell, T. J. McMahon, and D. G. Rathbun, J. appl. Phys. **39**, 48 (1968).
[16] R. K. Willardson and A. C. Beer, Semiconductors and Semimetals, Vol. **3**, Academic Press, Inc., London/New York 1967.
[17] T. J. McMahon, Ph. D. Dissertation, University of Missouri-Rolla, 1969.
T. J. McMahon and R. J. Bell, Phys. Rev. **182**, 526 (1969).
[18] R. N. Gamon and E. D. Palik, Surface Polariton Dispersion Relation and Damping Rate, to be published.
[19] J. J. Cowan, E. T. Arakawa, and R. H. Ritchie, Oak Ridge National Laboratory Report, ORNL-TM-2615.

(Received January 9, 1975)